HHS Public Access

Author manuscript

Pflugers Arch. Author manuscript; available in PMC 2022 November 01.

Published in final edited form as:

Pflugers Arch. 2018 February ; 470(2): 339–353. doi:10.1007/s00424-017-2084-x.

Dietary K^+ and Cl^- independently regulate basolateral conductance in principal and intercalated cells of the collecting duct

Viktor N. Tomilin[1], **Oleg Zaika**[1], **Arohan R. Subramanya**[2], **Oleh Pochynyuk**[1]

Oleh Pochynyuk: Oleh.M.Pochynyuk@uth.tmc.edu

[1]Department of Integrative Biology and Pharmacology, The University of Texas Health Science Center at Houston, 6431 Fannin, Houston, TX 77030, USA

[2]Department of Medicine, University of Pittsburgh School of Medicine, Pittsburgh, PA 15261, USA

Abstract

The renal collecting duct contains two distinct cell types, principal and intercalated cells, expressing potassium $K_{ir}4.1/5.1$ (KCNJ10/16) and chloride ClC-K2 (ClC-Kb in humans) channels on their basolateral membrane, respectively. Both channels are thought to play important roles in controlling systemic water-electrolyte balance and blood pressure. However, little is known about mechanisms regulating activity of $K_{ir}4.1/5.1$ and ClC-K2/b. Here, we employed patch clamp analysis at the single channel and whole cell levels in freshly isolated mouse collecting ducts to investigate regulation of $K_{ir}4.1/5.1$ and ClC-K2/b by dietary K^+ and Cl^- intake. Treatment of mice with high K^+ and high Cl^- diet (6% K^+, 5% Cl^-) for 1 week significantly increased basolateral K^+-selective current, single channel $K_{ir}4.1/5.1$ activity and induced hyperpolarization of basolateral membrane potential in principal cells when compared to values in mice on a regular diet (0.9% K^+, 0.5% Cl^-). In contrast, basolateral Cl^--selective current and single channel ClC-K2/b activity was markedly decreased in intercalated cells under this condition. Substitution of dietary K^+ to Na^+ in the presence of high Cl^- exerted a similar inhibiting action of ClC-K2/b suggesting that the channel is sensitive to variations in dietary Cl^- per se. Cl^--sensitive with-no-lysine kinase (WNK) cascade has been recently proposed to orchestrate electrolyte transport in the distal tubule during variations of dietary K^+. However, co-expression of WNK1 or its major downstream effector Ste20-related proline-alanine-rich kinase (SPAK) had no effect on ClC-Kb over-expressed in Chinese hamster ovary (CHO) cells. Treatment of mice with high K^+ diet without concomitant elevations in dietary Cl^- (6% K^+, 0.5% Cl^-) elicited a comparable increase in basolateral K^+-selective current, single channel $K_{ir}4.1/5.1$ activity in principal cells, but had no significant effect on ClC-K2/b activity in intercalated cells. Furthermore, stimulation of aldosterone signaling by Deoxycorticosterone acetate (DOCA) recapitulated the stimulatory actions of high K^+ intake on $K_{ir}4.1/5.1$ channels in principal cells but was ineffective to alter

---

Viktor N. Tomilin and Oleg Zaika contributed equally to this work.

Topical Collection on Ion channels, receptors and transporters

Compliance with ethical standards Animal use and welfare adhered to the NIH Guide for the Care and Use of Laboratory Animals following protocols reviewed and approved by the Animal Care and Use Committees of the University of Texas Health Science Center at Houston.

Conflict of interest The authors declare that they have no conflict of interest.

ClC-K2/b activity and basolateral Cl^- conductance in intercalated cells. In summary, we report that variations of dietary K^+ and Cl^- independently regulate basolateral potassium and chloride conductance in principal and intercalated cells. We propose that such discrete mechanism might contribute to fine-tuning of urinary excretion of electrolytes depending on dietary intake.

Keywords

K_{ir}4.1/5.1; ClC-K2/b; Principal and intercalated cells; WNK; Aldosterone; Distal tubule transport

Introduction

The kidneys are central in the regulation of systemic homeostasis and blood pressure control [15]. The final adjustments of water and electrolyte reabsorption occur in the collecting duct system in response to dietary intake and endocrine inputs [36]. Here, principal cells mediate epithelial Na^+ channel (ENaC)-mediated sodium reabsorption coupled to renal outer medullary K^+ channel (ROMK)-dependent potassium secretion [25, 36]. Electrically uncoupled intercalated cells are responsible for secretion of H^+ and HCO_3^- and trans-cellular Cl^- reabsorption [30, 36, 41]. Major effort has been put towards the investigation of signaling determinants that regulate apical membrane proteins [25], whereas much less is known about the mechanisms controlling basolateral membrane conductance in the collecting duct by endocrine and dietary cues.

Inwardly rectifying K_{ir}4.1 (KCNJ10) and K_{ir}5.1 (KCNJ16) form a functional heteromer, which is the major potassium channel on the basolateral membrane of the distal convoluted tubule and the collecting duct principal cells [17, 18, 51, 53]. Functional coupling of K_{ir}4.1/5.1 and Na^+/K^+-ATPase allows potassium recycling across the basolateral membrane, thereby setting the basolateral membrane potential to drive Na^+ reabsorption and K^+ secretion in the collecting duct [43, 49, 53]. Loss-of-function K_{ir}4.1 mutations underlie SeSAME/EAST syndrome in humans leading to urinary salt wasting, hypocalciuria, hypomagnesemia, and hypokalemic metabolic alkalosis [5, 33].

Basolateral Cl^- exit in intercalated cells is almost completely ClC-K2/b-dependent [10, 23]. ClC-K2/b is expressed in the kidney on the basolateral membrane from the thick ascending limb to the collecting duct [10, 16]. Coupling of ClC-K2/b with apical Cl^-/HCO_3^- exchangers Slc4a11 (in acid secreting A-type) and pendrin (Slc26a4 in base-secreting B-type) mediates transcellular Cl^- reabsorption in intercalated cells of the collecting duct [47]. Loss-of-function mutations of ClC-Kb or its auxiliary subunit barttin cause Bartter's syndrome in humans associated with in urinary salt wasting, hypochloremia, and low blood pressure [1, 4, 35].

Functional interplay between K_{ir}4.1/5.1 and ClC-K2/b expressed in the same distal convoluted tubule cells has been recently demonstrated to play a critical role in the adaptation to changes of dietary K^+ intake. K_{ir}4.1-dependent hyperpolarization of the basolateral membrane augments a driving force for the basolateral Cl^- exit via ClC-K2/b [39]. Recent observations suggest that reduced intracellular Cl^- concentration ($[Cl^-]_i$), as a result of ClC-K2/b activity, leads to activation of Cl^--sensitive with-no-lysine kinases

(WNK1 and WNK4) and their downstream Ste20-related proline-alanine-rich kinase (SPAK), which activate the electroneutral thiazide-sensitive Na-Cl cotransporter (NCC, Slc12a3) thereby reducing NaCl delivery to the collecting duct [38, 39]. Gain-of-function mutations in WNK1 and WNK4 cause familial hyperkalemic hypertension in humans (FHHt, also known as pseudohypoladosteronism type II or Gordon syndrome) [45]. It is striking that the basolateral membrane conductance of principal cells is virtually K^+-selective, whereas intercalated cells possess Cl^--selective basolateral exit [22] indicating the possibility of independent regulation of ion fluxes across electrically uncoupled principal and intercalated cells in response to local or systemic stimuli.

In this study, we subjected mice to diets with different content of K^+ and Cl^- to investigate how it affects $K_{ir}4.1/5.1$- and ClC-K2/b-dependent basolateral conductance in freshly isolated collecting ducts. Our results show that increased dietary amounts of K^+ and Cl^- elicited specific responses by stimulating $K_{ir}4.1/5.1$ in principal cells and inhibiting ClC-K2/b in intercalated cells, respectively. We also did not find a contribution of the WNK/SPAK pathway in the control of ClC-Kb activity. Thus, unlike the previously reported functional interplay in distal convoluted tubule cells, $K_{ir}4.1/5.1$ and ClC-K2/b are regulated independently in different cell types of the collecting duct in response to dietary KCl, pointing to a distinct segment-specific contribution of these channels to kidney function.

Materials and methods

Reagents and animals

All chemicals and materials were from Sigma (St. Louis, MO), VWR (Radnor, PA), and Tocris (Ellisville, MO) unless noted otherwise and were at least of reagent grade. Animal use and welfare adhered to the NIH Guide for the Care and Use of Laboratory Animals following protocols reviewed and approved by the Animal Care and Use Committees of the University of Texas Health Science Center at Houston. For experiments, male C57BL/6J mice (Charles River Laboratories, Wilmington, MA), 6–10 weeks old, were used. To examine effects of dietary potassium and chloride intake, animals were provided chow containing regular (0.9% K^+, 0.5% Cl^- 7012), high potassium high chloride (6% K^+, 5% Cl^-, TD.150699), high sodium high chloride (1.6% Na^+ and 2.4% Cl^-, TD.92034), and high potassium regular chloride (6% K^+, 0.5% Cl^-, TD.150759) for 7 days. The later diet was formulated to contain approximately 6% K^+ by adding 80.5 g potassium carbonate and 19.5 g potassium citrate per kg of diet. All diets were nutritionally balanced and were purchased from Envigo (Madison, WI, USA). As necessary for experimental design, mice were injected with Deoxycorticosterone acetate (DOCA, 2.4 mg/injection/animal) or olive oil as vehicle for 3 consecutive days prior to the experimentation, as we similarly did before [20, 21].

Tissue isolation

The procedure for isolation of the collecting ducts suitable for electrophysiology followed previously published protocols [48, 49, 51]. Briefly, mice were sacrificed by CO_2 administration followed by cervical dislocation, and the kidneys were removed immediately. Kidneys were cut into thin slices (< 1 mm) with slices placed into ice-cold physiological

saline solution (PSS) containing (in mM) 150 NaCl, 5 KCl, 1 $CaCl_2$, 2 $MgCl_2$, 5 glucose, and 10 HEPES (pH 7.35). Straight cortical-to-medullary sectors, containing approximately 30–50 renal tubules, were isolated by micro-dissection using watchmaker forceps under a stereomicroscope. Isolated sectors were further incubated in PSS containing 0.8 mg/ml collagenase type I (Alfa Aesar, Ward Hill, MA 01835) and 5 mg/ml of dispase II (Roche Diagnostics, Mannheim, Germany) for 20 min at 37 °C followed by extensive washout with PSS. Individual collecting ducts were visually identified by their morphological features (pale color, coarse surface and, in some cases, bifurcations) and were mechanically isolated from the sectors by micro-dissection. Isolated collecting ducts were attached to a 5 × 5-mm cover glass coated with poly-L-lysine. A cover-glass containing a collecting duct was placed in a perfusion chamber mounted on an inverted Nikon Eclipse Ti microscope and perfused with PSS at room temperature. The samples were used within 1–2 h after isolation. For each experimental condition, collecting ducts from at least four different mice were analyzed.

Whole cell currents and membrane potential in isolated collecting ducts

Whole cell currents in collecting cells were measured under voltage-clamp conditions in the perforated-patch mode with GigaOhm seals formed on the basolateral membrane. All patch clamp data were acquired with an Axopatch 200B (Molecular Devices, Sunnyvale CA) patch clamp amplifier interfaced via a Digidata 1440 (Molecular Devices, Sunnyvale CA) to a computer running the pClamp 10.5 (Molecular Devices, Sunnyvale CA). The bath solution was as follows (in mM): 150 NaCl, 5 KCl, 1 $CaCl_2$, 2 $MgCl_2$, 5 glucose, and 10 HEPES (pH 7.35). Freshly made Amphotericin-B, 400 μM (Enzo Life Sciences, Farmingdale, NY) was dissolved in the pipette solution containing 150 mM KAcetate, 5 mM KCl, 2 mM $MgCl_2$, 10 mM HEPES (pH 7.35) by ultrasonication. Electrical recordings were made once the access resistance from the pipette to the cell interior falls to less than 15 MΩ, usually 5–10 min after achieving a pipette-to-membrane seal resistance of 5–10 GΩ. Capacity of individual principal cells was in average 15 pF and was manually compensated. Measurements of resting membrane voltage in collecting duct cells were made under current-clamp mode using the perforated-patch technique as was described previously [48, 51].

Single channel recordings in isolated collecting ducts

Single channel activity of $K_{ir}4.1/5.1$ and ClC-K2/b in collecting duct cells was determined in cell-attached patches on the basolateral membrane made under voltage-clamp conditions. Recording pipettes had resistances of 8–10 MΩ. Bath and pipette solutions were as follows (in mM): 150 NaCl, 5 mM KCl, 1 $CaCl_2$, 2 $MgCl_2$, 5 glucose, and 10 HEPES (pH 7.35) and 150 mM KCl, 2 mM $MgCl_2$, 10 mM Hepes (pH 7.35). In the cell-attached configuration, the actual voltage applied to a membrane patch (V_{patch}) is a sum of the pipette voltage and the resting basolateral membrane potential of principal ($V_{basolateral}$, which is close to −70 mV for principal and − 15 mV for intercalated cells, see Fig. 1d). Currents were low-pass filtered at 1 kHz with an eight-pole Bessel filter (Warner Instruments, Hamden, CT). Events were inspected visually prior to acceptance. Channel activity (NP_o) and open probability (P_o) were assessed using Clampfit 10.5. Channel activity in individual patches, defined as NP_o, was calculated using the following equation: $NP_o = (t_1 + 2\ t_2 + \ldots + nt_n)$, where N is the number of active channels ($K_{ir}4.1/5.1$ or ClC-K2/b) in a patch and t_n is the fractional open time spent at each of the observed current levels. P_o was calculated by dividing NP_o by

the number of active channels within a patch as defined by all-point amplitude histograms. For representation, current traces were filtered at 200 Hz and corrected for a slow baseline drifts as necessary.

Over-expression of ClC-Kb in Chinese hamster ovary cells

Chinese hamster ovary (CHO) cells were obtained from the American Type Culture Collection. These cells were maintained with standard culture conditions (Dulbecco's modified Eagle's medium + 10% fetal bovine serum, 37 °C, 5% CO_2). Overexpression of human ClC-Kb, barttin, SPAK, and different WNKs into CHO cells was performed by transfecting the appropriate expression plasmids using the Polyfect reagent (Qiagen, Valencia, CA) followed protocols as described previously [27, 28]. Transfected cells were identified by GFP fluorescence after co-expression with green fluorescent protein (GFP) cDNA. Electrophysiological experiments were performed 48–72 h after transfection. For studies, 0.7 μg/9.6 cm^2 of ClC-Kb cDNA and 0.5 μg/9.6 cm^2 of all other plasmids cDNA were used. Expression vectors encoding human ClC-Kb and barttin Y98A were a kind gift from Dr. V. Bhalla (Stanford University). Barttin mutant Y98A lacking proline-tyrosine (PY) motif was used to maximally enhance ClC-Kb expression on the plasma membrane [8]. The cDNA encoding L-WNK1 was described previously [31]. L-WNK1 L369F/L371F, a hyperactive L-WNK1 mutant lacking Cl^- inhibition [26], was generated by site-directed mutagenesis (QuikChange kit, Agilent). The SPAK cDNA was a gift from James A. McCormick (Oregon Health and Science University). Whole cell capacitance was routinely compensated and was approximately 9 pF for CHO cells. Series resistances, on average 2–5 MΩ, were also compensated. Currents were evoked with 1-s voltage step protocols from − 60 to + 40 mV. Bath and pipette solutions were as follows (in mM): 150 NaCl, 5 KCl, 1 $CaCl_2$, 2 $MgCl_2$, 5 glucose, and 10 HEPES (pH 7.35) and 150 KCl, 5 NaCl, 2 $MgCl_2$, 5 EGTA, 10 Hepes, 2 ATP, 0.1 GTP (pH 7.35), respectively. For low $[Cl^-]_i$ experiments, pipette solution was 130 KAcetate, 15 KCl, 5 NaCl, 2 $MgCl_2$, 5 EGTA, 10 Hepes, 2 ATP, 0.1 GTP.

Data analysis

All summarized data are reported as mean ± SEM. Respective data sets were compared with a Student's (two-tailed) *t* test or a one-way ANOVA as appropriate. $P < 0.05$ was considered significant.

Results

Identification of principal and intercalated cells with patch clamp electrophysiology in freshly isolated collecting ducts

Collecting duct principal and intercalated cells have distinct transport properties and physiological roles [25, 30]. Our group as well as others reported that the basolateral membrane of principal cells exhibits virtually K^+-selective electrical conductance, mediated by $K_{ir}4.1/5.1$, and intercalated cells have ClC-K2/b mediated Cl^- current [10, 17, 23, 48, 49]. $K_{ir}4.1/5.1$ is essential to sustain Na^+/K^+ ATPase activity in order to drive apical Na^+ reabsorption and K^+ secretion in principal cells, while ClC-K2/b governs trans-cellular Cl^- reabsorption in intercalated cells (Fig. 1a).

Using patch clamp technique in whole cell mode in freshly isolated mouse collecting ducts (Fig. 1b), we are able to clearly identify principal and intercalated cells based on their electrical properties in response to voltage step protocol shown in Fig. 1c. As can be seen from the respective current-voltage (I–V) relations, whole cell current demonstrates a noticeable rectification at negative voltages with a reversal around − 70 mV in principal cells (Fig. 1d). We previously reported that this current can be blocked by Ba^{2+} and Cs^{+}, suggesting its K^{+}-selective nature [49]. In contrast, intercalated cells have considerably smaller currents with a reversal potential of − 15 mV, which is close to that of Cl^{-}, considering physiological distribution of the ions (Fig. 1d).

High KCl diet augments $K_{ir}4.1/5.1$ but inhibits ClC-K2/b activity in the collecting duct

Recent experimental evidence suggested that $K_{ir}4.1/5.1$ serves as a potassium sensor in the distal convoluted tubule to control intracellular Cl^{-} via ClC-K2/b via changes in basolateral membrane voltage [7, 39]. Thus, we first aimed to determine how variations in dietary K^{+} and Cl^{-} affect activity of $K_{ir}4.1/5.1$ and ClC-K2/b expressed in the different cell types of the collecting duct. Treatment of mice with high KCl diet (6% K^{+}, 5% Cl^{-}) for 1 week increased the amplitude of the basolateral K^{+}-selective conductance in CD principal cells (Fig. 2a), when compared to that from mice kept on regular diet (0.9% K^{+}, 0.5% Cl^{-}). Furthermore, we detected a leftward shift of the I–V relations in collecting duct principal cells from mice on high KCl diet, indicative of hyperpolarization of the basolateral membrane (Fig. 2b). Consistently, membrane resting potential was significantly more negative during high KCl diet (Fig. 2c). We also detected a significantly higher activity of 40 pS $K_{ir}4.1/5.1$ at the single channel level (Fig. 2d) during high KCl diet. This increase was attributable to both augmented channel open probability (P_o, Fig. 2e) and the number of active channels per patch (N, Fig. 2f). Moreover, we observed an increased single channel amplitude (Fig. 2g), which is consistent with basolateral membrane hyperpolarization shown in Fig. 2b, c. Specifically, this increased the driving force for K^{+} movement across $K_{ir}4.1/5.1$, whereas the channel conductance, the slope of i–V dependence, remains unchanged.

At the same time, high KCl diet significantly reduced macroscopic Cl^{-}-selective currents in intercalated cells (Fig. 3a). We did not detect notable changes in the reversal potential at the respective I–V relations (Fig. 3b), suggesting that ClC-K2/b channels do not play a role in establishing trans-epithelial voltage but serve as a passive conductive pathway for basolateral Cl^{-} exit. Consistently, we observed a significantly lower single channel 10 pS ClC-K2/b activity (Fig. 3c), open probability (Fig. 3d), and the number of active channels per patch (Fig. 3e), when animals were treated with high KCl diet. The unitary channel amplitude was not different (Fig. 3f) reflecting no apparent change of the basolateral voltage in intercalated cells from mice fed regular or high KCl diet (Fig. 3b).

Altogether, our results in Figs. 2 and 3 reveal that high KCl diet stimulates $K_{ir}4.1/5.1$-mediated potassium conductance in principal cells but inhibits ClC-K2/b-dependent basolateral Cl^{-} exit in intercalated cells.

High NaCl diet decreases basolateral conductance in both principal and intercalated cells

We next tested whether the opposite effects of high KCl diet on ClC-K2/b and $K_{ir}4.1/5.1$ reflect coordinated actions of the same mechanism or they are attributable to independent variations of dietary K^+ and Cl^- per se. Animals were given high NaCl diet (1.6% Na^+ and 2.4% Cl^-) for 1 week to recapitulate the state of high Cl^- and regular K^+ intake. When comparing to control condition (0.3% Na^+ and 0.5% Cl^-), we detected a decreased amplitude of the basolateral K^+-selective conductance in CD principal cells (Fig. 4a), a rightward shift of the respective I–V relation (Fig. 4b), and significantly more depolarized resting membrane potential (Fig. 4c). Both control and high NaCl diets contain identical levels of potassium (0.9% K^+). Single channel $K_{ir}4.1/5.1$ were also decreased (Fig. 4d) due to reduced channel open probability (P_o, Fig. 4e) and the number of active channels per patch (N, Fig. 4f). A reduced single channel amplitude (Fig. 4g) reflected a diminished driving force for K^+ due to membrane depolarization, while the channel conductance, the slope, remained constant.

Similarly to the observed effects induced by high KCl diet (Fig. 3), high NaCl diet substantially diminished macroscopic Cl^--selective currents in intercalated cells (Fig. 5a, b). Consistently, we detected a significantly lower single channel 10 pS ClC-K2/b activity (Fig. 5c), reduced open probability (Fig. 5d), and decreased number of active channels per patch (Fig. 5e), when compared to the values obtained in animals on control diet. The unitary channel amplitude was not different (Fig. 5f) indicating no measurable changes of the basolateral voltage during both conditions (Fig. 5b).

Overall, we concluded that basolateral ClC-K2/b Cl^- conductance in intercalated cells is regulated by dietary Cl^- independently of accompanying cation. NaCl-dependent reduction and KCl-induced stimulation of $K_{ir}4.1/5.1$ activity in principal cells point to a potential role of aldosterone cascade in regulation channel function during these states.

Evidence that ClC-K2/b is not a target of L-WNK1 or SPAK

Cl^--sensitive WNK/SPAK cascade has been implicated in maintaining of Cl^- homeostasis and regulation of cell volume [12, 44]. Thus, we next tested whether ClC-K2/b activity can be regulated by WNK/SPAK cascade. For this, we employed over-expression of human ClC-Kb into CHO cells. Transfection of ClC-Kb cDNA alone produced only a barely detectable macroscopic Cl^- current, when compared to non-transfected cells (Fig. 6a). In contrast, co-expression of ClC-Kb with its accessory barttin subunit increased current more than 10 times (Fig. 6b), which is consistent with the previously reported critical role of barttin in ClC-K2/b trafficking to the plasma membrane [32]. Thus, we expressed ClC-Kb with barttin in all following experiments.

Co-expression of full length kinase WNK1 (L-WNK1) did not produce any measurable effect on ClC-Kb macroscopic current, as shown in Fig. 6c. Bath and intracellular solutions had symmetrical 160 mM Cl^- in these experiments. To test whether the lack of an effect of L-WNK1 on ClC-Kb-dependent current might be explained by a baseline inhibition of L-WNK1 activity by high intracellular Cl^-, we next performed experiments when $[Cl^-]_i$ was clamped to a low level of 25 mM, a concentration which is insufficient to block WNK1

(IC_{50} ~ 40 mM) [26]. As expected, we observed a substantial leftward shift of the I–V relation, reflecting a new reversal potential for Cl^- (Fig. 6d). However, co-expression of WNK1 failed to affect ClC-Kb-mediated current in this condition (Fig. 6d). Moreover, we also did not find any measurable effect upon co-expression of WNK1 L369F/L371F mutant (Fig. 6e), an over-active L-WNK1 mutant which was reported to abolish inhibition of WNK1 by Cl^-[26, 39]. We next over-expressed SPAK to exclude the possibility that WNK1 fails to affect ClC-Kb when SPAK is not present. However, SPAK did not affect whole cell ClC-Kb current, when intracellular Cl^- was clamped to 25 mM (Fig. 6f). Altogether, the experiments in Fig. 6 suggest that inhibition of ClC-K2/b activity by high KCl diet likely occurs in a WNK/SPAK-independent manner.

Diet enriched in K^+ augments $K_{ir}4.1/5.1$ but has no effect on ClC-K2/b activity in the collecting duct

Our results (Figs. 3 and 5) suggest that basolateral Cl^- conductance in intercalated cells is regulated by dietary Cl^- irrespective of accompanying K^+ or Na^+. We next tested whether basolateral K^+ conductance in principal cells can be regulated independently from changes in conductance of intercalated cells. For this, animals were provided a diet with high K^+ (6% K^+), but regular Cl^- (0.5% Cl^-) for 1 week. As shown in Fig. 7, high K^+ diet exhibited a stimulatory action on $K_{ir}4.1/5.1$, when compared to the regular KCl diet. Specifically, we detected larger amplitudes of macroscopic K^+-selective currents (Fig. 7a, b), leftward shift of the I–V (Fig. 7b), and hyperpolarization of the basolateral membrane (Fig. 7c). At the single channel level, we observed a higher activity of the 40 pS $K_{ir}4.1/5.1$ channel (Fig. 7d) due to increased open probability (Fig. 7e) and the number of active channels per patch (Fig. 7f). Higher unitary current amplitude (Fig. 7g) is consistent with hyperpolarization of the basolateral plasma membrane, as detected in Fig. 7c. Overall, high KCl (Fig. 2) and high K^+ regular Cl^- (Fig. 7) diets exert comparable stimulatory effects on $K_{ir}4.1/5.1$ suggesting that this effect is dependent on dietary K^+ but not Cl^-.

On the contrary, high dietary K^+ fails to affect the activity of ClC-K2/b in the absence of concomitant elevations in dietary Cl^- (Fig. 8). Specifically, we did not detect any significant changes in the amplitude of Cl^--selective macroscopic current (Fig. 8a) and respective I–V relation (Fig. 8b) in intercalated cells of the collecting duct. Furthermore, single channel ClC-K2/b activity was comparable in mice fed with regular KCl diet and mice fed with high K^+ and regular Cl^- diet (Fig. 8c–f). These results further support the view that ClC-K2/b activity is sensitive to variations in dietary Cl^- but not K^+.

$K_{ir}4.1/5.1$ but not ClC-K2/b is sensitive to mineralocorticoids

Aldosterone is the principal hormone affecting transport rates in both principal and intercalated cells during variations in dietary electrolyte intake by targeting mineralocorticoid receptors (MR) [34, 36]. Thus, we tested how stimulation of aldosterone-MR cascade affects basolateral conductance in CD cells. Repetitive DOCA injections for 3 days significantly increased the amplitude of macroscopic K^+-selective currents compared to the values in vehicle injected mice (Fig. 9a, b) and induced hyperpolarization of the basolateral membrane of principal cells (Fig. 9c). Consistently, we detected a comparable upregulation of single channel $K_{ir}4.1/5.1$ activity in DOCA-injected animals (Fig. 9d–g).

In contrast, we failed to observe a measurable effect of DOCA on the macroscopic Cl^- conductance (Fig. 10a, b) and single channel ClC-K2/b activity (Fig. 10c–f) in intercalated cells. Overall, our data demonstrate that aldosterone exhibits specific stimulatory actions on the basolateral conductance of principal cells only likely participating in regulation of $K_{ir}4.1/5.1$ activity during variations in dietary K^+ intake.

Discussion

The collecting duct is different from other tubular segments (except the connecting tubule) with respect to containing heterogeneous cell population with different function and morphology [36]. Consistently, our patch clamp studies from freshly isolated collecting ducts identified two separate types of electrical responses, namely K^+-selective and Cl^--selective (Fig. 1), reflecting principal and intercalated cells, respectively. As we reported previously, whole cell currents in principal cells represent basolateral K^+-selective current sensitive to selective $K_{ir}4.1$ blocker, nortriptyline [24, 37]. This is due to much higher conductance of the basolateral compared to the apical membrane [9]. The contribution of apical conductance in whole cell current from intercalated cells is also very unlikely, since they do not possess notable electrogenic Cl^- selective conductance on the apical membrane. Furthermore, we and others demonstrated that activity of $K_{ir}4.1/5.1$ and ClC-K2/b underlie the basolateral macroscopic K^+ and Cl^- conductance, respectively, with little or no contamination by other channels [10, 17, 23, 48–51]. This gave us an advantage in correlating the effects of dietary K^+ and Cl^- on the electrical properties of the collecting duct at both single channel and whole cell levels. We found that increased K^+-selective current in principal cells by high K^+ diet (Figs. 2 and 7) and decreased Cl^--selective current in intercalated cells by high Cl^- diet (Figs. 3 and 8) is associated with respective changes in not only gating kinetics (open probability, P_o of $K_{ir}4.1/5.1$ and ClC-K2/b) but also the number of functional channels on the basolateral membrane potentially indicating complex mechanisms involving trafficking and/or transcription events. Additional carefully controlled studies are necessary to precisely dissect the mechanisms and molecular pathways responsible for the regulation of the basolateral channels in the collecting duct by dietary electrolytes.

As a part of the aldosterone-sensitive distal nephron, the collecting duct is a target of multiple hormones, including aldosterone and Angiotensin II [3, 19]. Thus, it is quite possible that alterations in dietary K^+ and Cl^- control $K_{ir}4.1/5.1$ and ClC-K2/b in the collecting duct by affecting levels of circulating hormones. Dietary K^+ loading (as a result of both high KCl and high K^+ regular Cl^- diets used in this study) increase circulating levels of the mineralocorticoid aldosterone to stimulate Na^+/K^+ exchange by increasing ENaC-mediated sodium reabsorption and K^+ secretion in principal cells [36]. Stimulatory effects of aldosterone on the apical ROMK and maxi-K (BK) channels and basolateral Na^+-K^+ ATPase have been also reported [42]. Our results (Figs. 2 and 7) show a significant upregulation of the basolateral $K_{ir}4.1/5.1$ channels in principal cells in mice treated with high KCl and high K^+ alone. Increased $K_{ir}4.1/5.1$ activity would further aid the Na^+/K^+ exchange by promoting Na^+-K^+ ATPase-dependent Na^+ exit and hyperpolarizing the basolateral membrane to favor apical K^+ secretion via ROMK and BK. We also found that stimulation of aldosterone cascade with DOCA augments $K_{ir}4.1/5.1$ (Fig. 9) pointing to its potential role in regulation

of the basolateral K^+ conductance in principal cells during variations in dietary K^+. In addition, aldosterone-independent mechanisms of K^+ secretion via WNK/SPAK have been also demonstrated [39]. However, transgenic mice expressing over-active WNK4 mutant causing pseudohypoladosteronism type II have unchanged $K_{ir}4.1$ activity in the distal convoluted tubule [52]. Further studies are necessary to examine the relative contribution and supremacy of aldosterone-dependent and -independent mechanisms in regulation of $K_{ir}4.1/5.1$ by dietary K^+.

On the contrary, aldosterone does not seem to play a role in regulation of ClC-K2/b activity in the collecting duct. We report here that stimulation of mineralocorticoid receptors with DOCA does not change macroscopic Cl^- conductance and single channel ClC-K2/b activity in intercalated cells (Fig. 10). A specific phosphorylation of mineralocorticoid receptors (S843-P), blocking ligand binding and activation, is found exclusively in intercalated cells [34]. Moreover, hyperkalemia augments S843-P phosphorylation, further precluding activation of mineralocorticoid receptors in intercalated cells during high K^+ diet condition. Consistently, we found that ClC-K2/b activity remained intact when animals were treated high K^+ regular Cl^- diet (Fig. 8), but inhibited by increased dietary Cl^- (Fig. 3). The mechanisms responsible for such Cl^- sensing remain enigmatic. Recent discovery of the inhibitory Cl^- binding pocket in WNKs implicated that these kinases, via sensing of $[Cl^-]_i$, play critical roles in a variety of physiological processes, such as cell volume regulation and maintaining Cl^- homeostasis [12, 44]. The measured $[Cl^-]_i$ in intercalated cells is 40–50 mM [6]. At these intracellular chloride concentrations, L-WNK1 would be expected to be highly sensitive to subtle changes in $[Cl^-]_i$, while WNK4 should be inactive [38]. Despite these prior observations, our results in CHO cells failed to establish a functional connection between ClC-K2/b, L-WNK1 and one of its major downstream effector kinases, SPAK (Fig. 5). This finding, however, does not necessarily exclude a role of the WNK/SPAK pathway in ClC-K2/b regulation, since putative additional components of this pathway might be missing in over-expression systems.

The major finding of this study is that basolateral $K_{ir}4.1/5.1$ and ClC-K2/b channels in the collecting duct can be independently regulated by dietary intake of potassium and chloride. Previous studies demonstrate that collecting duct principal and intercalated cells are electrically uncoupled [22, 46]. Furthermore, ClC-K2/b channel is located on the basolateral membrane of intercalated cells only [16, 23, 40], whereas $K_{ir}4.1/5.1$ expression is restricted to the basolateral membrane of principal cells [17, 49, 51]. Thus, it is reasonable to propose that such architecture is instrumental for independent movement of different ions across these cell types. Historically, the collecting duct is considered as a site where final adjustments of ENaC-mediated Na^+-reabsorption are coupled to K^+ secretion in principal cells [36]. However, increased ENaC activity in response to dietary potassium loading and to hypovolemia leads to discrete patterns of urinary excretion: kaliuresis with no volume retention and volume retention with little or no K^+ wasting, respectively, giving rise to the so-called “aldosterone paradox” [2]. A contributing factor could be that the apical Na^+ entry via ENaC in principal cells creates a favorable electrochemical gradient which can be used to drive potassium secretion, as well as paracellular and transcellular Cl^- reabsorption in intercalated cells [25, 36]. A commonly used high K^+ diet (which is also a high Cl^- diet) would lead to stimulation of $K_{ir}4.1/5.1$ activity and inhibition of ClC-K2/b-dependent Cl^-

reabsorption, thereby switching the collecting duct to a "K^+-secreting mode." Alternatively, a low Na^+ diet (which is also a low Cl^- diet) permits concomitant Na^+ and Cl^- reabsorption (i.e., volume retention) thus decreasing a driving force for K^+ secretion in the collecting duct. Of interest, this might be a common mechanism to dissociate ion fluxes in the collecting duct. Thus, we recently found that insulin, known for its pro-kaliuretic actions [11, 29], inhibits ClC-K2/b in murine collecting duct [48]. In contrast, insulin growth factor-1 (IGF-1), which can induce ENaC-dependent hypertension [13, 14], stimulates ClC-K2/b in intercalated cells [48].

In summary, we found a previously unrecognized regulation of collecting duct basolateral conductance and specifically $K_{ir}4.1/5.1$ and ClC-K2/b channels by dietary K^+ and Cl^-.

Since both channels play essential role in regulation of tubular transport and kidney function, they are attractive candidates for developing novel classes of diuretics to correct disturbances in water-electrolyte balance and blood pressure. Targeting their activity with pharmacological tools would have additional benefits of independent control of ion fluxes across principal and intercalated cells of the collecting duct, enabling more precise tuning of urinary excretion.

Acknowledgments

This research was supported by NIH-NIDDK DK095029 (to O. P.), AHA 17GRNT33660488 (to O. P.), NIH-NIDDK DK098145 (to A.R.S.), and ASN Ben J. Lipps Research Fellowship (to V. T.).

References

1. Andrini O, Keck M, Briones R, Lourdel S, Vargas-Poussou R, Teulon J. 2015; ClC-K chloride channels: emerging pathophysiology of Bartter syndrome type 3. Am J Physiol Ren Physiol. 308: F1324–F1334.
2. Arroyo JP, Ronzaud C, Lagnaz D, Staub O, Gamba G. 2011; Aldosterone paradox: differential regulation of ion transport in distal nephron. Physiology (Bethesda). 26: 115–123. [PubMed: 21487030]
3. Beutler KT, Masilamani S, Turban S, Nielsen J, Brooks HL, Ageloff S, Fenton RA, Packer RK, Knepper MA. 2003; Long-term regulation of ENaC expression in kidney by angiotensin II. Hypertension. 41: 1143–1150. [PubMed: 12682079]
4. Birkenhager R, Otto E, Schurmann MJ, Vollmer M, Ruf EM, Maier-Lutz I, Beekmann F, Fekete A, Omran H, Feldmann D, Milford DV, Jeck N, Konrad M, Landau D, Knoers NV, Antignac C, Sudbrak R, Kispert A, Hildebrandt F. 2001; Mutation of BSND causes Bartter syndrome with sensorineural deafness and kidney failure. Nat Genet. 29: 310–314. [PubMed: 11687798]
5. Bockenhauer D, Feather S, Stanescu HC, Bandulik S, Zdebik AA, Reichold M, Tobin J, Lieberer E, Sterner C, Landoure G, Arora R, Sirimanna T, Thompson D, Cross JH, van't Hoff W, Al Masri O, Tullus K, Yeung S, Anikster Y, Klootwijk E, Hubank M, Dillon MJ, Heitzmann D, Arcos-Burgos M, Knepper MA, Dobbie A, Gahl WA, Warth R, Sheridan E, Kleta R. 2009; Epilepsy, ataxia, sensorineural deafness, tubulopathy, and KCNJ10 mutations. N Engl J Med. 360: 1960–1970. [PubMed: 19420365]
6. Boettger T, Hubner CA, Maier H, Rust MB, Beck FX, Jentsch TJ. 2002; Deafness and renal tubular acidosis in mice lacking the K-cl co-transporter KCC4. Nature. 416: 874–878. [PubMed: 11976689]
7. Cuevas CA, Su XT, Wang MX, Terker AS, Lin DH, McCormick JA, Yang CL, Ellison DH, Wang WH. 2017; Potassium sensing by renal distal tubules requires $K_{ir}4.1$. J Am Soc Nephrol : JASN. 28: 1814–1825. [PubMed: 28052988]

8. Estevez R, Boettger T, Stein V, Birkenhager R, Otto E, Hildebrandt F, Jentsch TJ. 2001; Barttin is a cl^- channel beta-subunit crucial for renal cl^- reabsorption and inner ear K^+ secretion. Nature. 414: 558–561. [PubMed: 11734858]
9. Gray DA, Frindt G, Zhang YY, Palmer LG, Basolateral K. 2005; $^+$ conductance in principal cells of rat CCD. Am J Physiol Ren Physiol. 288: F493–F504.
10. Hennings JC, Andrini O, Picard N, Paulais M, Huebner AK, Cayuqueo IK, Bignon Y, Keck M, Corniere N, Bohm D, Jentsch TJ, Chambrey R, Teulon J, Hubner CA, Eladari D. 2017; The ClC-K2 Chloride Channel is critical for salt handling in the distal nephron. J Am Soc Nephrol: JASN. 28: 209–217. [PubMed: 27335120]
11. Hoekstra M, Yeh L, Lansink AO, Vogelzang M, Stegeman CA, Rodgers MG, van der Horst IC, Wietasch G, Zijlstra F, Nijsten MW. 2012; Determinants of renal potassium excretion in critically ill patients: the role of insulin therapy. Crit Care Med. 40: 762–765. [PubMed: 21946656]
12. Kahle KT, Rinehart J, de Los Heros P, Louvi A, Meade P, Vazquez N, Hebert SC, Gamba G, Gimenez I, Lifton RP. 2005; WNK3 modulates transport of Cl^- in and out of cells: implications for control of cell volume and neuronal excitability. Proc Natl Acad Sci U S A. 102: 16783–16788. [PubMed: 16275911]
13. Kamenicky P, Blanchard A, Frank M, Salenave S, Letierce A, Azizi M, Lombes M, Chanson P. 2011; Body fluid expansion in acromegaly is related to enhanced epithelial sodium channel (ENaC) activity. J Clin Endocrinol Metab. 96: 2127–2135. [PubMed: 21508131]
14. Kamenicky P, Viengchareun S, Blanchard A, Meduri G, Zizzari P, Imbert-Teboul M, Doucet A, Chanson P, Lombes M. 2008; Epithelial sodium channel is a key mediator of growth hormone-induced sodium retention in acromegaly. Endocrinology. 149: 3294–3305. [PubMed: 18388193]
15. Khawaja Z, Wilcox CS. 2011; Role of the kidneys in resistant hypertension. Int J Hypertens. 2011: 143471. [PubMed: 21461391]
16. Kobayashi K, Uchida S, Mizutani S, Sasaki S, Marumo F. 2001; Intrarenal and cellular localization of CLC-K2 protein in the mouse kidney. J Am Soc Nephrol: JASN. 12: 1327–1334. [PubMed: 11423561]
17. Lachheb S, Cluzeaud F, Bens M, Genete M, Hibino H, Lourdel S, Kurachi Y, Vandewalle A, Teulon J, Paulais M. 2008; $K_{ir}4.1/K_{ir}5.1$ channel forms the major K^+ channel in the basolateral membrane of mouse renal collecting duct principal cells. Am J Physiol Ren Physiol. 294: F1398–F1407.
18. Lourdel S, Paulais M, Cluzeaud F, Bens M, Tanemoto M, Kurachi Y, Vandewalle A, Teulon J. 2002; An inward rectifier K^+ channel at the basolateral membrane of the mouse distal convoluted tubule: similarities with $K_{ir}4$-$K_{ir}5.1$ heteromeric channels. J Physiol. 538: 391–404. [PubMed: 11790808]
19. Makhanova N, Lee G, Takahashi N, Sequeira Lopez ML, Gomez RA, Kim HS, Smithies O. 2006; Kidney function in mice lacking aldosterone. Am J Physiol Ren Physiol. 290: F61–F69.
20. Mamenko M, Zaika O, Prieto MC, Jensen VB, Doris PA, Navar LG, Pochynyuk O, Chronic Angiotensin II. 2013; Infusion drives extensive aldosterone-independent epithelial Na+ channel activation. Hypertension. 62: 1111–1122. [PubMed: 24060890]
21. Mamenko MV, Boukelmoune N, Tomilin VN, Zaika OL, Jensen VB, O'Neil RG, Pochynyuk OM. 2017; The renal TRPV4 channel is essential for adaptation to increased dietary potassium. Kidney Int. 91: 1398–1409. [PubMed: 28187982]
22. Muto S, Yasoshima K, Yoshitomi K, Imai M, Asano Y. 1990; Electrophysiological identification of alpha- and beta-intercalated cells and their distribution along the rabbit distal nephron segments. J Clin Invest. 86: 1829–1839. [PubMed: 2254448]
23. Nissant A, Paulais M, Lachheb S, Lourdel S, Teulon J. 2006; Similar chloride channels in the connecting tubule and cortical collecting duct of the mouse kidney. Am J Physiol Ren Physiol. 290: F1421–F1429.
24. Ohno Y, Hibino H, Lossin C, Inanobe A, Kurachi Y. 2007; Inhibition of astroglial $K_{ir}4.1$ channels by selective serotonin reuptake inhibitors. Brain Res. 1178: 44–51. [PubMed: 17920044]
25. Pearce D, Soundararajan R, Trimpert C, Kashlan OB, Deen PM, Kohan DE. 2014. Collecting duct principal cell transport processes and their regulation. Clin J Am Soc Nephrol: CJASN.

26. Piala AT, Moon TM, Akella R, He H, Cobb MH, Goldsmith EJ. 2014; Chloride sensing by WNK1 involves inhibition of autophosphorylation. Science Signaling. 7: ra41. [PubMed: 24803536]
27. Pochynyuk O, Kucher V, Boiko N, Mironova E, Staruschenko A, Karpushev AV, Tong Q, Hendron E, Stockand J. 2009. Intrinsic voltage-dependence of the epithelial Na+ channel is masked by a conserved transmembrane domain tryptophan. J Biol Chem.
28. Pochynyuk O, Tong Q, Medina J, Vandewalle A, Staruschenko A, Bugaj V, Stockand JD. 2007; Molecular determinants of PI(4,5)P_2 and PI(3,4,5)P_3 regulation of the epithelial Na+ channel. J Gen Physiol. 130: 399–413. [PubMed: 17893193]
29. Rossetti L, Klein-Robbenhaar G, Giebisch G, Smith D, DeFronzo R. 1987; Effect of insulin on renal potassium metabolism. Am J Phys. 252: F60–F64.
30. Roy A, Al-bataineh MM, Pastor-Soler NM. 2015; Collecting duct intercalated cell function and regulation. Clin J Am Soc Nephrol: CJASN. 10: 305–324. [PubMed: 25632105]
31. Roy A, Al-Qusairi L, Donnelly BF, Ronzaud C, Marciszyn AL, Gong F, Chang YP, Butterworth MB, Pastor-Soler NM, Hallows KR, Staub O, Subramanya AR. 2015; Alternatively spliced proline-rich cassettes link WNK1 to aldosterone action. J Clin Invest. 125: 3433–3448. [PubMed: 26241057]
32. Scholl U, Hebeisen S, Janssen AG, Muller-Newen G, Alekov A, Fahlke C. 2006; Barttin modulates trafficking and function of ClC-K channels. Proc Natl Acad Sci U S A. 103: 11411–11416. [PubMed: 16849430]
33. Scholl UI, Choi M, Liu T, Ramaekers VT, Hausler MG, Grimmer J, Tobe SW, Farhi A, Nelson-Williams C, Lifton RP. 2009; Seizures, sensorineural deafness, ataxia, mental retardation, and electrolyte imbalance (SeSAME syndrome) caused by mutations in KCNJ10. Proc Natl Acad Sci U S A. 106: 5842–5847. [PubMed: 19289823]
34. Shibata S, Rinehart J, Zhang J, Moeckel G, Castaneda-Bueno M, Stiegler AL, Boggon TJ, Gamba G, Lifton RP. 2013; Mineralocorticoid receptor phosphorylation regulates ligand binding and renal response to volume depletion and hyperkalemia. Cell Metab. 18: 660–671. [PubMed: 24206662]
35. Simon DB, Bindra RS, Mansfield TA, Nelson-Williams C, Mendonca E, Stone R, Schurman S, Nayir A, Alpay H, Bakkaloglu A, Rodriguez-Soriano J, Morales JM, Sanjad SA, Taylor CM, Pilz D, Brem A, Trachtman H, Griswold W, Richard GA, John E, Lifton RP. 1997; Mutations in the chloride channel gene, CLCNKB, cause Bartter's syndrome type III. Nat Genet. 17: 171–178. [PubMed: 9326936]
36. Staruschenko A. 2012; Regulation of transport in the connecting tubule and cortical collecting duct. Compr Physiol. 2: 1541–1584. [PubMed: 23227301]
37. Su S, Ohno Y, Lossin C, Hibino H, Inanobe A, Kurachi Y. 2007; Inhibition of astroglial inwardly rectifying K_{ir}4.1 channels by a tricyclic antidepressant, nortriptyline. J Pharmacol Exp Ther. 320: 573–580. [PubMed: 17071817]
38. Terker AS, Zhang C, Erspamer KJ, Gamba G, Yang CL, Ellison DH. 2016; Unique chloride-sensing properties of WNK4 permit the distal nephron to modulate potassium homeostasis. Kidney Int. 89: 127–134. [PubMed: 26422504]
39. Terker AS, Zhang C, McCormick JA, Lazelle RA, Zhang C, Meermeier NP, Siler DA, Park HJ, Fu Y, Cohen DM, Weinstein AM, Wang WH, Yang CL, Ellison DH. 2015; Potassium modulates electrolyte balance and blood pressure through effects on distal cell voltage and chloride. Cell Metab. 21: 39–50. [PubMed: 25565204]
40. Uchida S, Sasaki S. 2005; Function of chloride channels in the kidney. Annu Rev Physiol. 67: 759–778. [PubMed: 15709977]
41. Wall SM, Weinstein AM. 2013; Cortical distal nephron cl^- transport in volume homeostasis and blood pressure regulation. Am J Physiol Ren Physiol. 305: F427–F438.
42. Wang WH, Giebisch G. 2009; Regulation of potassium handling in the renal collecting duct. Pflugers Archiv : Eur J Physiol. 458: 157–168. [PubMed: 18839206]
43. Wang WH, Yue P, Sun P, Lin DH. 2010; Regulation and function of potassium channels in aldosterone-sensitive distal nephron. Curr Opin Nephrol Hypertens. 19: 463–470. [PubMed: 20601877]
44. Watanabe M, Fukuda A. 2015; Development and regulation of chloride homeostasis in the central nervous system. Front Cell Neurosci. 9: 371. [PubMed: 26441542]

45. Wilson FH, Disse-Nicodeme S, Choate KA, Ishikawa K, Nelson-Williams C, Desitter I, Gunel M, Milford DV, Lipkin GW, Achard JM, Feely MP, Dussol B, Berland Y, Unwin RJ, Mayan H, Simon DB, Farfel Z, Jeunemaitre X, Lifton RP. 2001; Human hypertension caused by mutations in WNK kinases. Science. 293: 1107–1112. [PubMed: 11498583]
46. Woda CB, Leite M Jr, Rohatgi R, Satlin LM. 2002; Effects of luminal flow and nucleotides on $[Ca^{2+}]_i$ in rabbit cortical collecting duct. Am J Physiol Ren Physiol. 283: F437–F446.
47. Xu J, Barone S, Li H, Holiday S, Zahedi K, Soleimani M. 2011; Slc26a11, a chloride transporter, localizes with the vacuolar H^+-ATPase of a-intercalated cells of the kidney. Kidney Int. 80: 926–937. [PubMed: 21716257]
48. Zaika O, Mamenko M, Boukelmoune N, Pochynyuk O. 2015; IGF-1 and insulin exert opposite actions on ClC-K2 activity in the cortical collecting ducts. Am J Physiol Ren Physiol. 308: F39–F48.
49. Zaika O, Palygin O, Tomilin V, Mamenko M, Staruschenko A, Pochynyuk O. 2016; Insulin and IGF-1 activate K_{ir}4.1/5.1 channels in cortical collecting duct principal cells to control basolateral membrane voltage. Am J Physiol Ren Physiol. 310: F311–F321.
50. Zaika O, Tomilin V, Mamenko M, Bhalla V, Pochynyuk O. 2016; New perspective of ClC-kb/2 cl-channel physiology in the distal renal tubule. Am J Physiol Ren Physiol. 310: F923–F930.
51. Zaika OL, Mamenko M, Palygin O, Boukelmoune N, Staruschenko A, Pochynyuk O. 2013; Direct inhibition of basolateral K_{ir}4.1/5.1 and K_{ir}4.1 channels in the cortical collecting duct by dopamine. Am J Physiol Ren Physiol. 305: F1277–F1287.
52. Zhang C, Wang L, Su XT, Zhang J, Lin DH, Wang WH. 2017; ENaC and ROMK activity are inhibited in the DCT2/CNT of TgWnk4PHAII mice. Am J Physiol Ren Physiol. 312: F682–F688.
53. Zhang C, Wang L, Zhang J, Su XT, Lin DH, Scholl UI, Giebisch G, Lifton RP, Wang WH. 2014; KCNJ10 determines the expression of the apical Na-Cl cotransporter (NCC) in the early distal convoluted tubule (DCT1). Proc Natl Acad Sci U S A. 111: 11864–11869. [PubMed: 25071208]

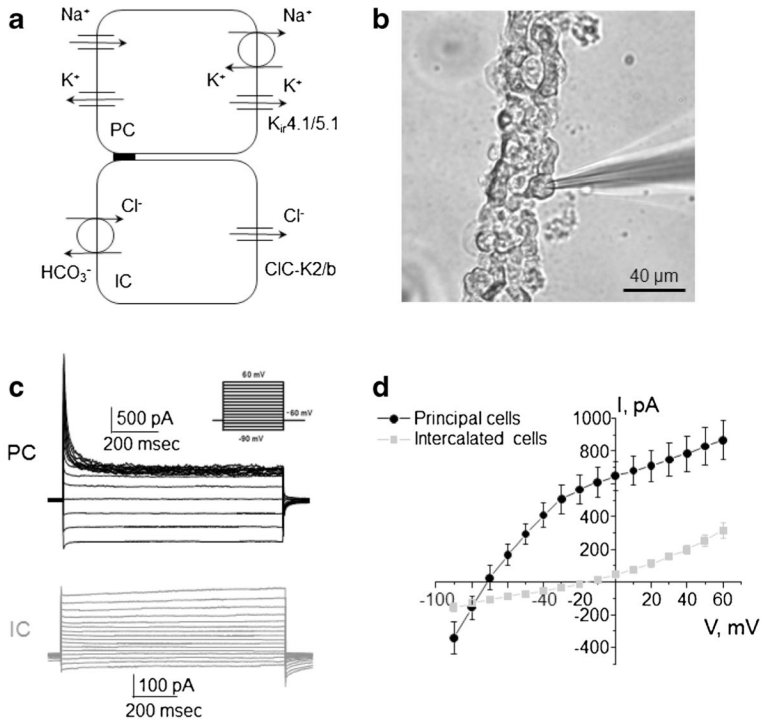

Fig. 1. Separation of electrical signals from principal and intercalated cells of the mouse collecting duct

a Schematic representation of principal and intercalated cells (PC and IC, respectively) showing major routs of Na^+, K^+, and Cl^- movement. Acid-secreting (A-type) and base secreting (B-type) intercalated cells are combined for reasons of simplification. **b** Representative micrograph of a typical freshly isolated collecting duct enzymatically treated to expose the basolateral membrane for patch clamp assessment. **c** Two discrete types of electrical responses to voltage steps from − 90 to + 60 mV (shown in inset) from the holding potential of − 60 mV from experiments similar to shown in **b. d** Averaged current-voltage (I–V) relations of principal cells having K^+-selective conductance (black) and intercalated cells exhibiting Cl^--sensitive current (gray)

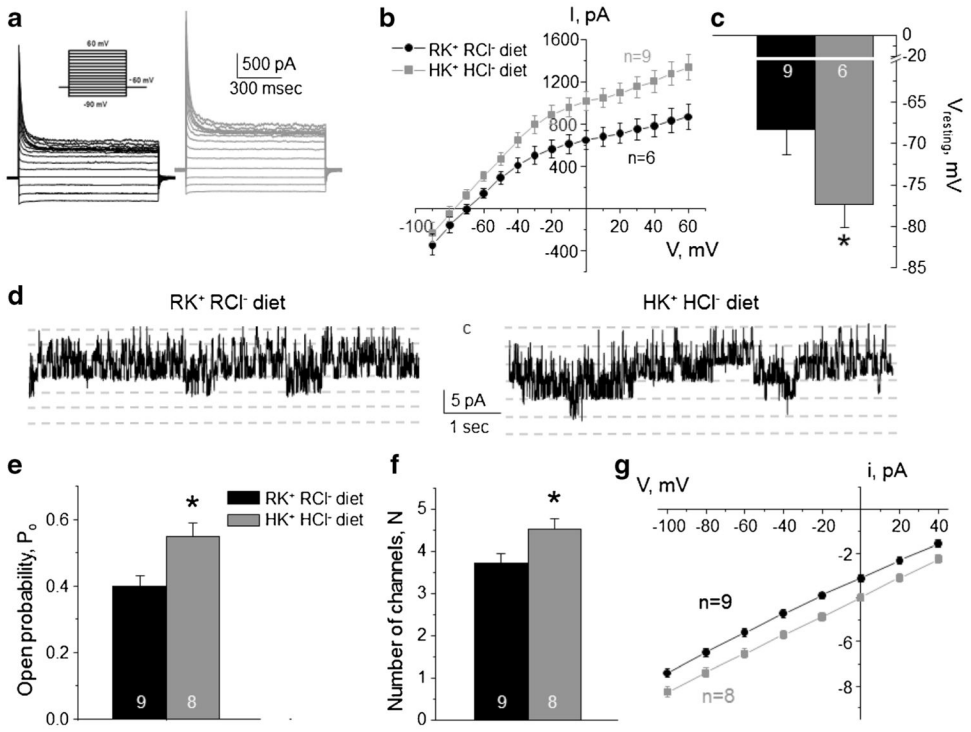

Fig. 2. High K^+ high Cl^- diet increases K_{ir}4.1/5.1 activity on the basolateral membrane of collecting duct principal cells

Representative macroscopic currents in response to voltage steps from − 90 to + 60 mV (shown in inset) from the holding potential of − 60 mV (**a**), averaged current-voltage (I–V) relations (**b**), and the summary graph of resting basolateral membrane potential (**c**) in principal cells from mice kept on regular diet (0.9% K^+, 0.5% Cl^-: RK^+ RCl^-, black) and high KCl diet (6% K^+, 5% Cl^-: HK^+ HCl^-, gray). **d** Representative continuous current traces from cell-attached patches monitoring basolateral 40 pS K_{ir}4.1/5.1 single channel activity in collecting duct principal cells for the regular (left) and high KCl (right) conditions. Patches were clamped to $-V_p = -40$ mV. “C” denotes non-conducting closed state. Summary graph of changes in open probability (**e**), number of active channels within a patch (**f**), and unitary current amplitude (**g**) of K_{ir}4.1/5.1 in principal cells from mice on regular diet and high KCl diet. *Significant difference versus regular diet

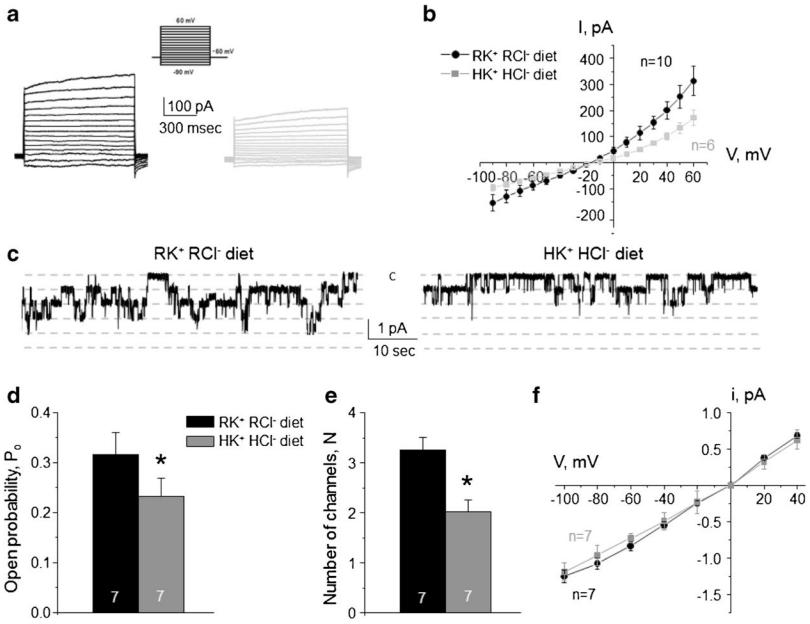

Fig. 3. High K^+ high Cl^- diet decreases ClC-K2/b activity on the basolateral membrane of collecting duct intercalated cells

Representative macroscopic currents in response to voltage steps from −90 to + 60 mV (shown in inset) from the holding potential of − 60 mV (**a**) and averaged current-voltage (I–V) relations (**b**) in intercalated cells from mice kept on regular diet (0.9% K^+, 0.5% Cl^-: RK^+ RCl^-, black) and high KCl diet (6% K^+, 5% Cl^-: HK^+ HCl^-, gray). **c** Representative continuous current traces from cell-attached patches monitoring basolateral 10 pS ClC-K2/b single channel activity in collecting duct intercalated cells for the regular (left) and high KCl (right) conditions. Patches were clamped to $-V_p = -60$ mV. "C" denotes non-conducting closed state. Summary graph of changes in open probability (**d**), number of active channels within a patch (**e**), and unitary current amplitude (**f**) of ClC-K2/b in intercalated cells from mice on regular diet and high KCl diet. *Significant difference versus regular diet

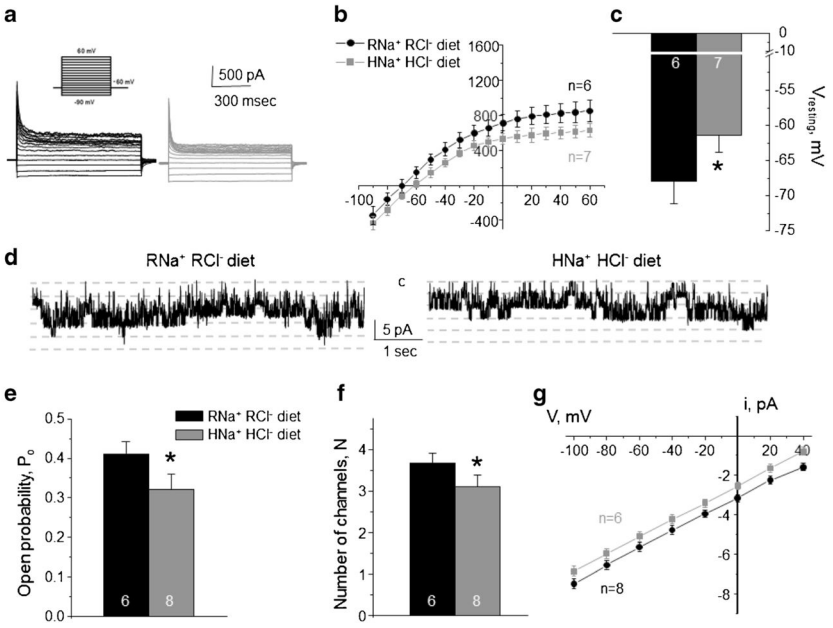

Fig. 4. High Na^+ high Cl^- diet inhibits basolateral K^+ conductance and $K_{ir}4.1/5.1$ activity in collecting duct principal cells

Representative macroscopic currents in response to voltage steps from − 90 to + 60 mV (shown in inset) from the holding potential of − 60 mV (**a**), averaged current-voltage (I–V) relations (**b**), and the summary graph of resting basolateral membrane potential (**c**) in principal cells from mice kept on regular diet (0.3% Na^+, 0.5% Cl^-: RNa^+ RCl^-, black) and high NaCl diet (1.6% Na^+, 2.4% Cl^-: HNa^+ HCl^-, gray). **d** Representative continuous current traces from cell-attached patches monitoring basolateral 40 pS $K_{ir}4.1/5.1$ single channel activity in collecting duct principal cells for the regular (left) and high NaCl (right) conditions. Patches were clamped to $-V_p$ = − 40 mV. “C” denotes non-conducting closed state. Summary graph of changes in open probability (**e**), number of active channels within a patch (**f**), and unitary current amplitude (**g**) of $K_{ir}4.1/5.1$ in principal cells from mice on regular diet and high NaCl diet. *Significant difference versus regular diet

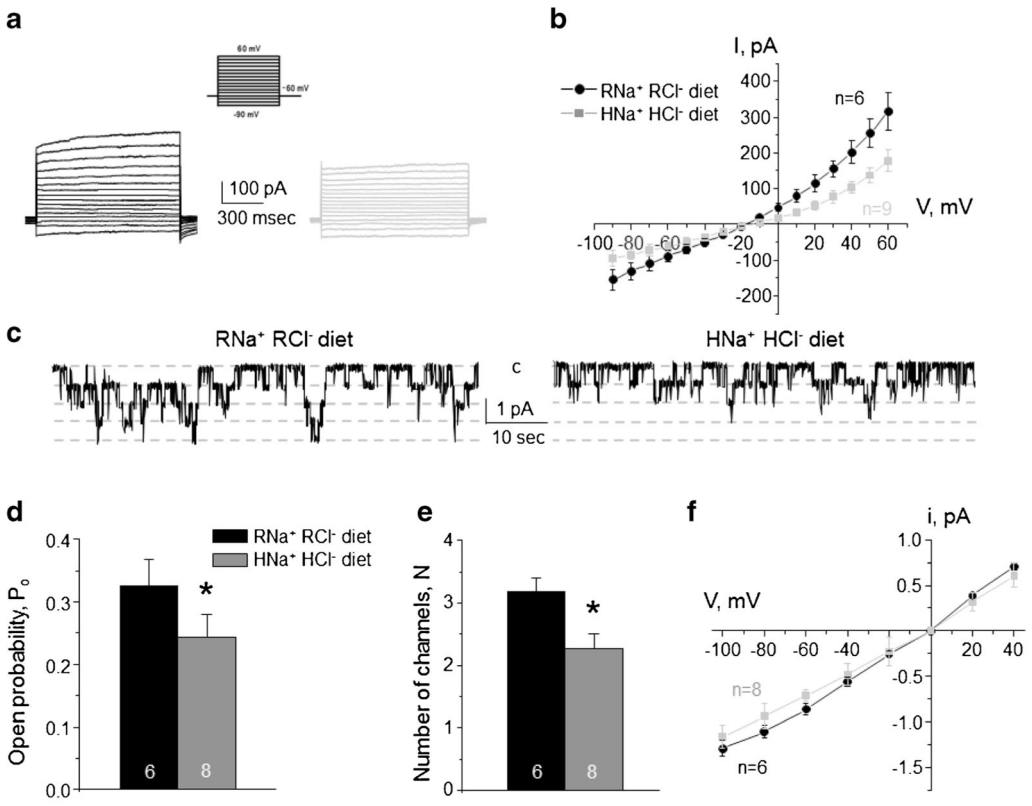

Fig. 5. High Na^+ high Cl^- diet decreases ClC-K2/b activity on the basolateral membrane of collecting duct intercalated cells

Representative macroscopic currents in response to voltage steps from −90 to + 60 mV (shown in inset) from the holding potential of − 60 mV (**a**) and averaged current-voltage (I–V) relations (**b**) in intercalated cells from mice kept on regular diet (0.3% Na^+, 0.5% Cl^-: RNa^+ RCl^-, black) and high NaCl diet (1.6% Na^+, 2.4% Cl^-: HNa^+ HCl^-, gray). **c** Representative continuous current traces from cell-attached patches monitoring basolateral 10 pS ClC-K2/b single channel activity in collecting duct intercalated cells for the regular (left) and high NaCl (right) conditions. Patches were clamped to $-V_p = -60$ mV. "C" denotes non-conducting closed state. Summary graph of changes in open probability (**d**), number of active channels within a patch (**e**), and unitary current amplitude (**f**) of ClC-K2/b in intercalated cells from mice on regular diet and high NaCl diet. *Significant difference versus regular diet

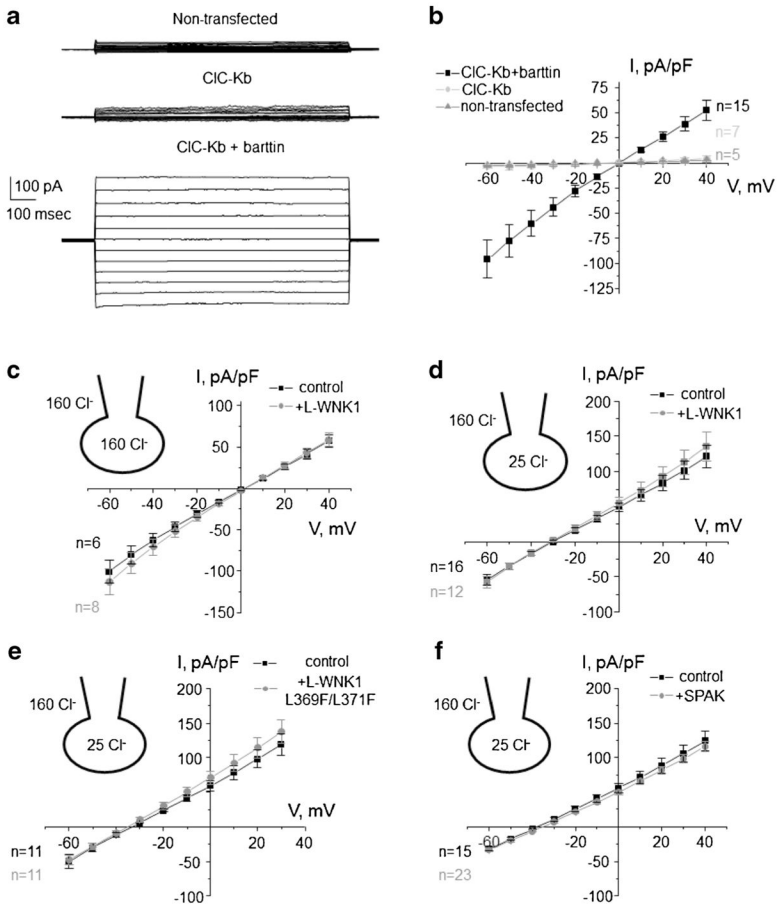

Fig. 6. WNK/SPAK do not regulate ClC-Kb activity over-expressed in CHO cells

a Representative macroscopic whole-cell currents in non-transfected cells (top), upon expression of ClC-Kb alone (middle), ClC-Kb + barttin evoked by series of voltage steps from − 60 to + 40 mV in CHO cells. **b** The averaged current-voltage (I–V) relations from experimental conditions in **a**. The averaged I–V relations of ClC-Kb + barttin in the absence (control) and presence of L-WNK1 co-expression in high intracellular Cl^- (**c**) and low intracellular Cl^- (**d**) conditions. The actual bath and pipette/cytosol Cl^- concentrations are shown in respective insets here and below. **e** The averaged (I–V) relations of ClC-Kb + barttin in the absence (control) and presence of Cl-binding site deficient L-WNK1 mutant (L-WNK1 L369F/L371F) co-expression. **f** The averaged I–V relations of ClC-Kb + barttin in the absence (control) and presence of SPAK. The numbers of individual experiments are also shown

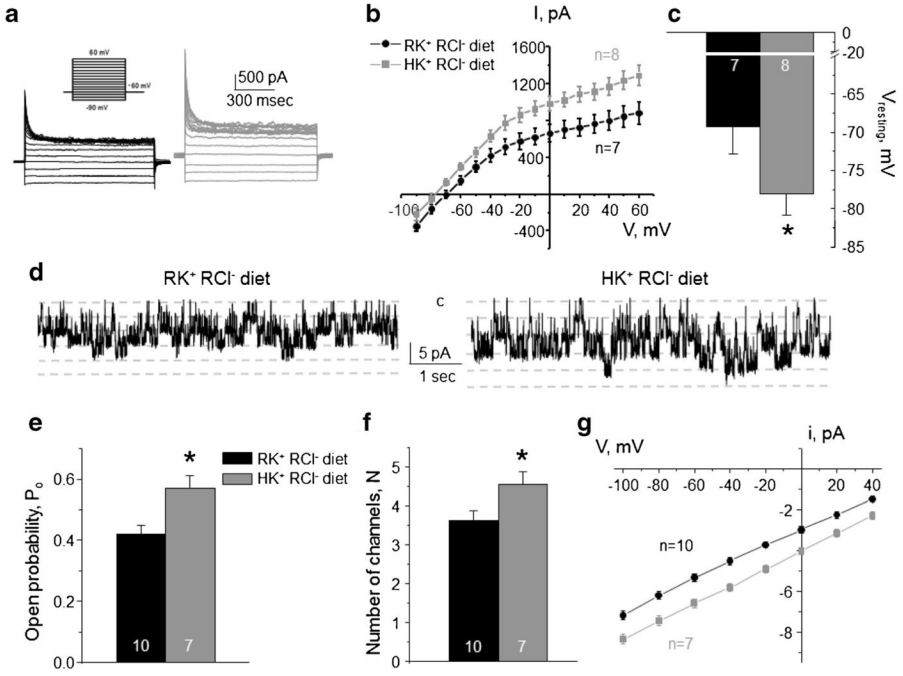

Fig. 7. High K^+ regular Cl^- diet increases $K_{ir}4.1/5.1$ activity on the basolateral membrane of collecting duct principal cells

Representative macroscopic currents in response to voltage steps from − 90 to + 60 mV (shown in inset) from the holding potential of − 60 mV (**a**), averaged current-voltage (I–V) relations (**b**), and the summary graph of resting basolateral membrane potential (**c**) in principal cells from mice kept on regular diet (0.9% K^+, 0.5% Cl^-: RK^+ RCl^-, black) and high K^+ regular Cl^- diet (6% K^+, 0.5% Cl^-: HK^+ RCl^-, gray). **d** Representative continuous current traces from cell-attached patches monitoring basolateral 40 pS $K_{ir}4.1/5.1$ single channel activity in collecting duct principal cells for the regular (left) and high K^+ (right) conditions. Patches were clamped to $-V_p = -40$ mV. “C” denotes non-conducting closed state. Summary graph of changes in open probability (**e**), number of active channels within a patch (**f**), and unitary current amplitude (**g**) of $K_{ir}4.1/5.1$ in principal cells from mice on regular diet and high K^+ regular Cl^- diet. *Significant difference versus regular diet

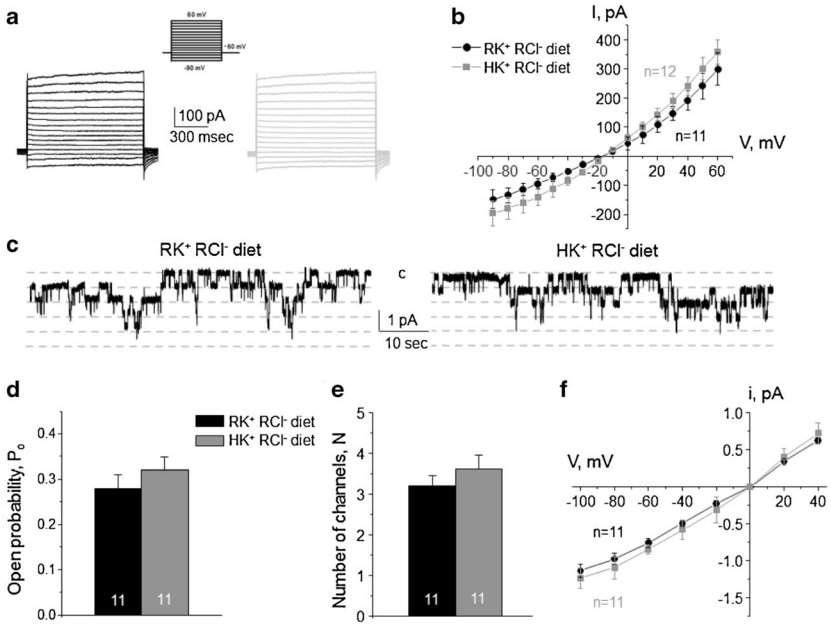

Fig. 8. High K^+ regular Cl^- diet has no effect on the basolateral ClC-K2/b channel in collecting duct intercalated cells

Representative macroscopic currents in response to voltage steps from − 90 to + 60 mV (shown in inset) from the holding potential of − 60 mV (**a**) and averaged current-voltage (I–V) relations (**b**) in intercalated cells from mice kept on regular diet (0.9% K^+, 0.5% Cl^-: RK^+ RCl^-, black) and high K^+ regular Cl^- diet (6% K^+, 0.5% Cl^-: HK^+ RCl^-, gray). **c** Representative continuous current traces from cell-attached patches monitoring basolateral 10 pS ClC-K2/b single channel activity in collecting duct intercalated cells for the regular (left) and high K^+ (right) conditions. Patches were clamped to $-V_p$ = − 60 mV. “C” denotes non-conducting closed state. Summary graph of changes in open probability (**d**), number of active channels within a patch (**e**), and unitary current amplitude (**f**) of ClC-K2/b in intercalated cells from mice on regular diet and high K^+ regular Cl^- diet

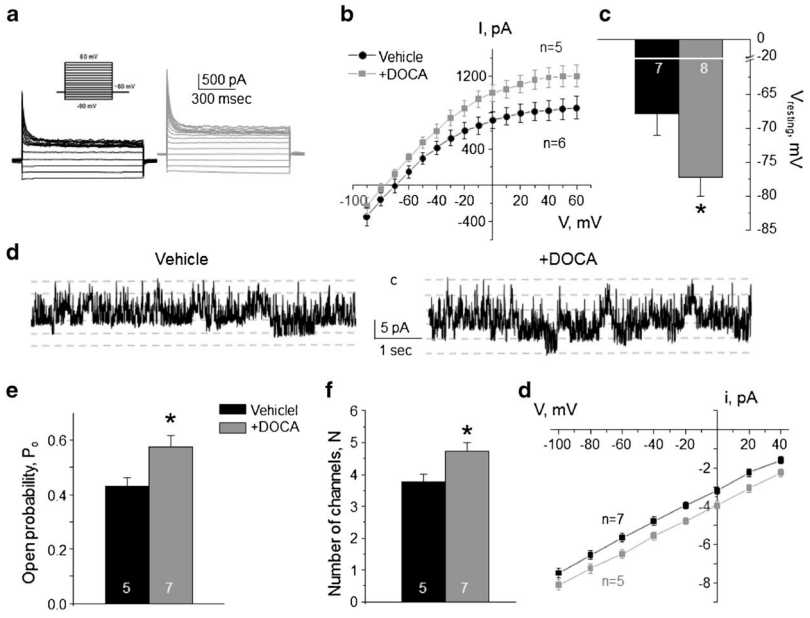

Fig. 9. Stimulation of aldosterone signaling with Deoxycorticosterone acetate (DOCA) increases K_{ir}4.1/5.1 activity on the basolateral membrane of collecting duct principal cells

Representative macroscopic currents in response to voltage steps from − 90 to + 60 mV (shown in inset) from the holding potential of − 60 mV (**a**), averaged current-voltage (I–V) relations (**b**), and the summary graph of resting basolateral membrane potential (**c**) in principal cells from mice repetitively injected with vehicle (black) and DOCA (gray) for 3 days. **d** Representative continuous current traces from cell-attached patches monitoring basolateral 40 pS K_{ir}4.1/5.1 single channel activity in collecting duct principal cells from vehicle (left) and DOCA (right) injected mice. Patches were clamped to $-V_p$ = − 40 mV. “C” denotes non-conducting closed state. Summary graph comparing open probability (**e**), number of active channels within a patch (**f**), and unitary current amplitude (**g**) of K_{ir}4.1/5.1 in principal cells in mice receiving vehicle and DOCA. *Significant difference versus vehicle

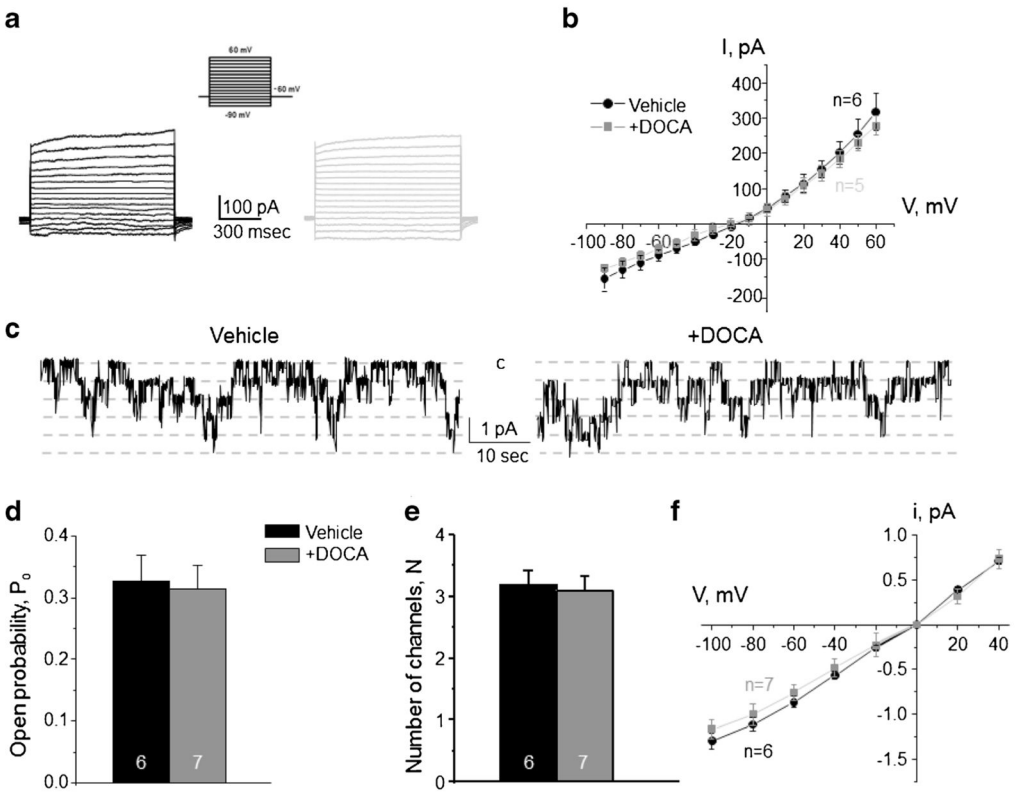

Fig. 10. Deoxycorticosterone acetate (DOCA) injections fail to affect the basolateral Cl^- conductance in collecting duct intercalated cells

Representative macroscopic currents in response to voltage steps from −90 to + 60 mV (shown in inset) from the holding potential of − 60 mV (**a**) and averaged current-voltage (I–V) relations (**b**) in intercalated cells from mice injected with vehicle (black) and DOCA (gray) for 3 consecutive days. **c** Representative continuous current traces from cell-attached patches monitoring basolateral 10 pS ClC-K2/b single channel activity in collecting duct intercalated cells for the vehicle (left) and DOCA (right) conditions. Patches were clamped to $-V_p$ = − 60 mV. "C" denotes non-conducting closed state. Summary graph of changes in open probability (**d**), number of active channels within a patch (**e**), and unitary current amplitude (**f**) of ClC-K2/b in intercalated cells from mice subjected to vehicle and DOCA injections